Fracture characteristics of titanium VT1-0 and Zr–1 wt. % Nb alloy in different structures under gigacycle fatigue loading regime

Cite as: AIP Conference Proceedings **2051**, 020184 (2018); https://doi.org/10.1063/1.5083427
Published Online: 12 December 2018

A. Mairambekova, A. Eroshenko, M. Bannikov, O. Naimark, and Yu. Sharkeev

Fracture Characteristics of Titanium VT1-0 and Zr–1 wt. % Nb Alloy in Different Structures under Gigacycle Fatigue Loading Regime

A. Mairambekova[1,a)], A. Eroshenko[2,b)], M. Bannikov[3,c)], O. Naimark[3,d)], and Yu. Sharkeev[2,4,e)]

[1] *National Research Tomsk State University, Tomsk, 634050 Russia*
[2] *Institute of Strength Physics and Materials Science SB RAS, Tomsk, 634055 Russia*
[3] *Institute of Continuous Media Mechanics UrB RAS, Perm, 614013 Russia*
[4] *National Research Tomsk Polytechnic University, Tomsk, 634050 Russia*

[a)] Corresponding author: aikol@ispms.tsc.ru
[b)] eroshenko@ispms.tsc.ru
[c)] mbannikov@iccm.ru
[d)] naimark@icmm.ru
[e)] sharkeev@ispms.tsc.ru

Abstract. Fatigue testing of ultrafine-grained, fine-grained and coarse-grained VT1-0 and Zr–1 wt. % Nb samples was performed under conditions of gigacycle fatigue regime. It was established that ultrafine-grained titanium and zirconium alloy samples initiate increasing fatigue strength of up to 1.3 times for titanium and 1.7 times for zirconium alloy within gigacycle region (10^9 cycles) comparable to fine-grained and coarse-grained samples. Analysis of fracture surface morphology has revealed the similar fractured structure in coarse-grained and ultrafine-grained titanium and zirconium alloy samples. Fractures in ultrafine-grained titanium and zirconium alloy samples exhibit quasi-brittle pattern.

INTRODUCTION

Prevailing applicable alloys used in medicine are commercially pure titanium (VT1-0, VT1-00, Grade 1, 2, 3, 4) and titanium alloys (Ti–6Al–4V, Ti–6Al–4VELi, Ti–6Al–7Nb и Ti–6Al–2.5Fe) [1]. Due to high corrosion resistance zirconium alloys Zr–1Nb, Zr–2.5Nb (commercial alloys E110 and E125) are applied as structural material in nuclear power industry [2] and medicine. A limited factor for the widespread application of commercially pure titanium and zirconium alloys as implant material is the low mechanical properties, including fatigue strength and cycle life. Producing bulk nanostructured (NS) and/or ultrafine-grained (UFG) structure in metals and alloys by severe plastic deformation (SPD) methods resulted in profound improvement of mechanical properties (yield strength, ultimate strength, hardness, fatigue limit, cyclic fatigue, etc.) [3]. It is a well-known fact that NS formation and UFG structures in metals effectively improves the wear resistance within the high-cycle fatigue region (more than 10^6 loading cycles) [4, 5]. Currently, the most pressing issues are to investigate the NS and/or UFG structure effect on material fracture under cyclic loading, to analyze the fatigue curve within a wide cycle loading range, including both high-cycle fatigue (10^6 loading cycles) and gigacycle loading (in the case of 10^9 loading cycles or more) [6–8].

The research aim is to determine the fracture characteristics of VT1-0 and Zr–1 wt. % Nb alloy in UFG and coarse-grained structures under loading cycles within gigacycle fatigue regime.

Proceedings of the Advanced Materials with Hierarchical Structure for New Technologies and Reliable Structures
AIP Conf. Proc. 2051, 020184-1–020184-4; https://doi.org/10.1063/1.5083427
Published by AIP Publishing. 978-0-7354-1777-9/$30.00

EXPERIMENTAL PROCEDURES

The investigated target was commercially pure titanium VT1-0 and E110 (Zr–1 wt. % Nb) alloy. The ultrafine-grained structure in investigated samples was produced in two-stage combined SPD method, which included abc-pressing and multi-pass rolling in grooved rollers with further recrystallization annealing [9]. Coarse-grained (CG) structure in titanium and fine-grained (FG) structure in zirconium alloy are produced by recrystallization annealing of UFG samples for 1 hour in a vacuum: at 800°C for titanium and 580°C for zirconium alloy. The microstructure and phase composition of the samples were investigated by optical microscopy (Carl Zeiss Axio Observer) scanning and transmission electronic microscopy (JEOL JEM 2100, LEO EVO 50). The average element structure size (grains, subgrains, fragments) was calculated by using linear secant method. Shimadzu USF-2000 ultrasonic fatigue testing machine was used to identify gigacycle fatigue at such given conditions: stress amplitude range of 100–300 MPa, cyclic oscillation frequency 20 kHz with asymmetry cycle coefficient $R = -1$ [8].

Cylindrical dogbone samples were produced from ultrafine-grained, coarse-grained and fine-grained titanium and zirconium alloy billet bars for fatigue testing. The geometrical sizes of the samples were determined by the analytic formulas [7, 8] in dependence of investigated material density and dynamic elastic (Young's) modulus to the conditions of standing-ultrasonic wave and resonant testing system. Air cooling was used to prevent high-temperature heating of the samples during fatigue testing.

RESULTS AND DISCUSSION

Ultrafine-grained titanium and zirconium alloy were produced by combined SPD method (Fig. 1). UFG microstructure was the characteristic feature of above-mentioned materials. Fragments and subgrains, as well as crystallized grains were observed. The boundaries of grains, subgrains and fragments were non-equilibrium. The distinctive microstructure feature was numerous extinction contours, showing the evidence of existing high residual elastic stress level (Figs. 1a, 1c). Highly dense dislocated substructure was localized in grains, subgrains and fragments. Average element structure size (grains, subgrains and fragments) was 0.2 ± 0.1 μm for titanium and 0.22 ± 0.1 μm for zirconium alloy. This corresponded in structure to UFG.

Numerous point reflexes of multi-varied intensity arranged along the circles were observed on both titanium and zirconium alloy microdiffraction patterns (Figs. 1a, 1b). This indicated existing large-angle and small-angle disorientation on grain and subgrain boundaries. Identified microdiffraction patterns for zirconium alloy (Fig. 1b) showed reflections of high intensity from α-Zr phase (hexagonal close-packed lattice) and low intensity from β-Nb phase (body-centered cubic lattice). It should be noted that no Nb particles was observed on bright-field images. Energy-dispersive X-ray spectroscopy of elemental composition was applied to identify β-Nb particles in phase. After recrystallization annealing titanium microstructure involved rather average equiaxial grains of 27 ± 8 μm (Fig. 1c). Recrystallized fine-grained zirconium alloy had α-Zr grain (average grain size of 1.9 ± 0.4 μm) and located on the boundaries Nb particles of average size 0.4 μm within matrix grain bodies (Fig. 1d).

Figure 2 illustrate the experimental points and fatigue curves for titanium and zirconium alloy of selected (UFG, CG, FG) structures. Arrows indicate the non-fractured samples during testing. At given stress amplitude 175 MPa, the coarse-grained titanium sample fractured after 10^5 cycles. Transformation from CG to UFG structure significantly improved titanium fatigue resistance within gigacycle fatigue region. At given stress amplitude 200 MPa the number of loading cycles before fracture increased to 1.9×10^9. According to fatigue testing results, the fatigue limit of coarse-grained titanium within 10^9 loading cycles was 155 MPa, while for ultrafine-grained titanium—200 MPa, which was 1.3 times more.

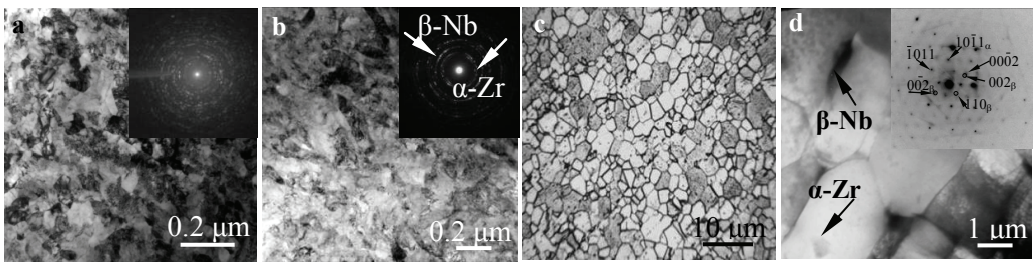

FIGURE 1. Titanium microstructure (a, c) and zirconium alloy (b, d) as UFG structure (a, b) and recrystallized structure (c, d): electron microscopic bright-field image (a, b, d) with corresponding microdifraction patterns; optical image (c)

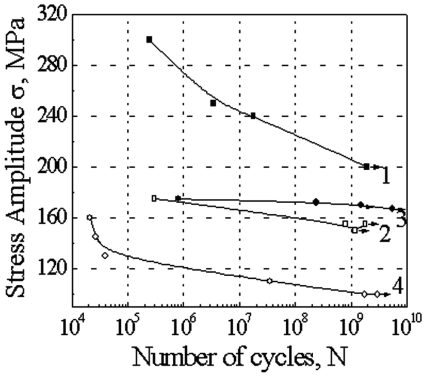

FIGURE 2. Fatigue curves (Weller's curves) for titanium and zirconium alloy in various structural states: ■—UFG titanium, curve *1*; □—coarse-grained titanium, curve *2*; ●—UFG zirconium alloy, curve *3*; ○—fine-grained zirconium alloy, curve *4*

Fatigue fracture of ultrafine-grained zirconium alloy was within low-cycle region ($N \le 2.1 \times 10^4$ cycles) at stress amplitude $\sigma = 160$ MPa. Fine-grained structure forming in zirconium alloy resulted in increasing fatigue resistance within gigacycle loading regime. The number of loading cycles before UFG zirconium alloy sample fracture was 1.5×10^9 cycles at stress 170 MPa. Fatigue limit for UFG zirconium alloy was 100 MPa, while for fine-grained zirconium alloy—1.7 times more, i.e. 160 MPa.

To study investigated material fatigue fracture characteristics, the comparative analysis of fracture surface morphology samples was performed. Titanium and zirconium alloy samples fractured within low-cycle fatigue region ($N \le 10^5$ cycles) embracing the stress amplitude range of 300–160 MPa were selected. In some cases, samples fracture surface could not be "revealed" in the course of resonant frequency changes (fatigue loading stoppage), dynamic break and preliminary sample cooling in liquid nitrogen.

There are three typical zones on all fatigue fracture surfaces: initiation and stable crack growth; subsequent crack growth; and upload failure zone [4]. Fatigue cracks originated close to the lateral surface and propagated inward in all samples.

Figures 3 and 4 illustrate SEM-images of fatigue fracture surface for titanium and zirconium alloy samples in different structures.

Initiation and crack growth (Figs. 3a, 3d) is characterized by near-perfect roughness and smooth micropatterns with fine cracks. Fracture microrelief included predominately comparable smooth and flat fragments. During transition from the initiation to the growth of cracks, simultaneous with smooth fragments and "tongue-like" fracture surface, "dimple" microrelief emerged, being typical of ductile fracture. Secondary cracks and numerous small pores were observed. Fatigue grooves (Figs. 3b, 3e) were visible in-situ zirconium alloy on smooth fragments. Failure zone was characterized by "dimple" microrelief (Figs. 3c, 3f).

Fracture surface within crack nucleus zone for coarse-grained titanium and fine-grained zirconium alloy revealed smooth microrelief with small cracks (Figs. 4a, 4d). In crack growth zone the fracture revealed a combined structure: visible surface areas with flat fragments and "tongue-like" fractures and "dimple" areas (Figs. 4b, 4d) indicating quasi-brittle pattern; no fatigue grooves for coarse-grained titanium and fine-grained zirconium alloy.

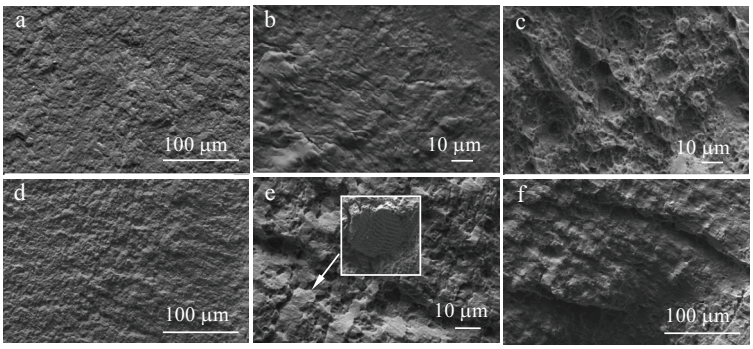

FIGURE 3. SEM-images of fracture surface for UFG titanium (a–c) and zirconium alloy (d–f) samples: (a, d) initiation and stable crack growth; (b, e) subsequent crack growth; (c, f) failure zone

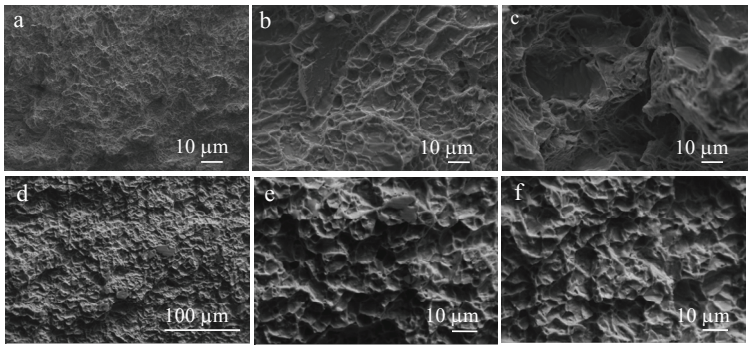

FIGURE 4. SEM-images of fracture surface for UFG (a, c) and CG (d, f) zirconium alloy: (a, d) initiation and stable crack growth; (b, e) subsequent crack growth; (c, f) failure zone

Fracture surface in crack propagation zone revealed numerous pores and secondary cracks. Sample fracture of coarse-grained titanium and fine-grained zirconium alloy within failure zone revealed mainly "dimple" microrelief (Figs. 4c, 4f).

CONCLUSIONS

High fatigue resistance was determined in gigacycle loading regimes for UFG titanium and zirconium alloy. UFG structure-forming resulted in increased fatigue limit: 1.3 times for titanium VT1-0 and 1.7 times for zirconium alloy Zr–1 wt. % Nb within gigacycle fatigue regime. Thus, morphology analysis of fatigue surface proved the fact that crack-like patterns were observed in coarse-grained and UFG titanium and zirconium alloy. Fracture of UFG titanium and zirconium alloy samples indicated quasi-brittle pattern.

ACKNOWLEDGMENTS

The research was performed by support of Russian Foundation for Basic Research, project 17-32-50163 (fatigue testing) and Fundamental Scientific Research Program of National Academy of Sciences 2017–2020, program 23.2 (microstructure investigation).

Experimental research was conducted on the financial equipments of Common Use Center "Nanotech" at Institute of Strength Physics and Materials Science SB RAS (ISPMS SB RAS, Tomsk, Russia).

Authors would like to thank PhD student V. Chebodaeva for her help in the performance of the experiments.

REFERENCES

1. M. Niinomi, M. Nakai, and J. Hieda, Acta Biomater. **8**, 3888–3903 (2012).
2. M. T. Mohammed, Z. A. Khan, and A. N. Siddiquee, Int. J. Chem. Mol. Nucl. Mater. Metall. Eng. **8**, 788.
3. R. Z. Valiev, A. P. Zhilyaev, and T. G. Langdon, *Bulk Nanostructured Materials: Fundamentals and Applications* (John Wiley, Hoboken, New Jersey, USA, 2014).
4. A. A. Shanyavsky, Phys. Mesomech. **18**(2), 163–173 (2015).
5. I. P. Semenova, R. Z. Valiev, E. B. Yakushina, G. H. Salimgareeva, and T. C. Lowe, J. Mater. Sci. **43**, 7354–7359 (2008).
6. H. Mughrabi, Int. J Fatigue **28**, 1501–1508 (2006).
7. V. I. Betekhtin, A. G. Kadomtsev, M. V. Narykova, M. V. Bannikov, S. G. Abaimov, I. Sh. Akhatov, T. Palin-Luc, and O. B. Naimark, Phys. Mesomech **20**(1), 78–89 (2017).
8. O. B. Naimark, Phys. Met. Metallogr. **84**, 327–337 (1997).
9. Yu. P. Sharkeev, A. Yu. Eroshenko, V. I. Danilov, A. I. Tolmachev, P. V. Uvarkin, and Yu. A. Abzaev, Russ. Phys. J. **56**, 1156–1162 (2014).